

Cilostazol Protects Rat Chondrocytes Against Nitric Oxide–Induced Apoptosis In Vitro and Prevents Cartilage Destruction in a Rat Model of Osteoarthritis

Sung Won Lee,¹ Yeon Suk Song,¹ Sang Hwa Shin,¹ Kyung Taek Kim,¹ Young Chul Park,²
Bong Soo Park,² Il Yun,² Kunhong Kim,³ Sang Yeob Lee,¹ Won Tae Chung,¹
Hye Jeong Lee,¹ and Young Hyun Yoo¹

Objective. To examine whether cilostazol, a selective phosphodiesterase type III inhibitor, protects rat articular chondrocytes against nitric oxide (NO)–induced apoptosis and prevents cartilage destruction in mono-iodoacetate–induced osteoarthritis (OA) in a rat model in which inducible nitric oxide synthase (iNOS) is expressed.

Methods. The NO donor sodium nitroprusside was administered to rat articular chondrocytes that had been pretreated with cilostazol. Induction of apoptosis was evaluated by DNA electrophoresis and pulsed-field gel electrophoresis. The expression level and the subcellular location of apoptosis-associated factors were examined by Western blot analysis and confocal microscopy, respectively. Protein kinase CK2 (PKCK2) activity was also assayed. To examine whether orally administered cilostazol prevents cartilage destruction in vivo, cartilage samples obtained from rats with experimentally induced OA were subjected to hematoxylin and eosin, Safranin O, and TUNEL staining and immunohistochemical analysis of iNOS expression.

Results. Cilostazol prevented NO-induced reduc-

tion in viability, in a dose-dependent manner. It also prevented the up-regulation of phosphorylated p53 and p38, the down-regulation of heme oxygenase 1, the subcellular translocation of apoptosis-inducing factor and cytochrome *c*, and the activation of caspases 3, 7, and 8 induced by NO treatment, indicating that cilostazol prevented NO-induced cell death by blocking apoptosis. In addition, cilostazol prevented NO-induced translocation of cleaved Bid onto mitochondria, and caused phosphorylated Bid to accumulate in the nucleus and cytosol. Cilostazol prevented the down-regulation of PKCK2 and the reduction in PKCK2 activity induced by NO, indicating that its apoptosis-preventing activity was mediated via PKCK2. It also prevented chondrocyte apoptosis and cartilage destruction in a rat model of experimentally induced OA.

Conclusion. Our findings indicate that cilostazol prevents NO-induced apoptosis of chondrocytes via PKCK2 in vitro and prevents cartilage destruction in a rat model of OA.

Osteoarthritis (OA) is characterized by degradation of matrix and destruction of articular cartilage (1). Articular chondrocytes are solely responsible for the production and maintenance of the extracellular matrix. Therefore, chondrocyte apoptosis is implicated in cartilage degeneration (2,3). Several stimuli, such as nitric oxide (NO) (4–7), prostaglandin E₂ (8), Fas ligand (9,10), tumor necrosis factor α (TNF α) (11), and TRAIL (12) have been reported to induce apoptosis in chondrocytes. Since those apoptosis-inducing substances might play a part in the pathogenesis of OA, manipulation of the mechanism mediated by those stimuli has the potential for substantial therapeutic impact.

NO is believed to be an important mediator of

Supported by the Korea Science and Engineering Foundation (grants R01-2004-000-10002-0 and R01-2007-000-20100-0).

¹Sung Won Lee, MD, PhD, Yeon Suk Song, MS, Sang Hwa Shin, MD, Kyung Taek Kim, MD, Sang Yeob Lee, MD, Won Tae Chung, MD, Hye Jeong Lee, MD, Young Hyun Yoo, MD, PhD: Dong-A University, Seo-Gu, Busan, South Korea; ²Young Chul Park, PhD, Bong Soo Park, PhD, Il Yun, PhD: Pusan National University, Seo-Gu, Busan, South Korea; ³Kunhong Kim, MD: Yonsei University, Seodaemun-Gu, Seoul, South Korea.

Address correspondence and reprint requests to Young Hyun Yoo, MD, PhD, Department of Anatomy and Cell Biology, Dong-A University College of Medicine, Medical Science Research Center, 3-1 Dongdaesin-Dong, Seo-Gu, Busan 602-7143, South Korea. E-mail: yhyoo@dau.ac.kr.

Submitted for publication May 16, 2007; accepted in revised form November 14, 2007.

the dedifferentiation and apoptosis of articular chondrocytes in arthritic cartilage (6). It is produced in chondrocytes by the action of proinflammatory cytokines such as interleukin-1 β . NO production in chondrocytes causes activation of matrix metalloproteinases (MMPs), decreased production of interleukin-1 β receptor antagonist, inhibition of proteoglycan synthesis and type II collagen expression, and apoptosis of chondrocytes (2,13,14).

Cilostazol, 6-[4-(1-cyclohexyl-1*H*-tetrazol-5-yl)butoxy]-3,4-dihydro-2-(1*H*)-quinolinone, is a potent selective phosphodiesterase type III (PDE III) inhibitor. It elevates intercellular cyclic cAMP by blocking its hydrolysis by PDE III (15). Cilostazol functions as a platelet aggregation inhibitor (15) and vasodilator (16), and is mainly used for treating patients with peripheral arterial disease (17) and intermittent claudication (18). In addition, it seems to reduce inflammation and inhibit MMP expression by increasing AMP and inhibiting the p38/JNK pathway (19). Previous studies have demonstrated that cilostazol inhibits apoptosis under several circumstances (12,20–22). In those studies, cilostazol was shown to prevent lipoprotein particle-induced apoptosis in human umbilical vein endothelial cells (HUVECs) (22), lipopolysaccharide-induced apoptosis in HUVECs (20), and ischemic injury-induced apoptosis in neural cells (12,21). Notably, protein kinase CK2 (PKCK2) was reported to be involved in the prevention of apoptosis by cilostazol (12,23).

PKCK2 has typically been classified as a messenger-independent protein serine/threonine kinase (24,25). It is distributed ubiquitously in the cell cytoplasm and nucleus of eukaryotic organisms. Although the role of PKCK2 is unknown, it may potentially participate in a complex series of cellular functions, including cell growth and proliferation, by catalyzing the phosphorylation of a large number of proteins (26). PKCK2 also participates in the regulation of apoptosis by phosphorylating some apoptosis-related factors (26–31). Despite the many previous studies of PKCK2, little progress has been made in understanding its molecular role in chondrocytes.

This study was undertaken to determine whether cilostazol prevents NO-induced chondrocyte apoptosis and to examine the role of PKCK2 in this effect. Our findings indicated that cilostazol protects rat chondrocytes against NO-induced apoptosis via PKCK2 *in vitro*, and that oral administration of cilostazol prevents cartilage destruction in rats with experimentally induced OA.

MATERIALS AND METHODS

Reagents. Rabbit polyclonal anti-human caspase 3, caspase 7, and cytochrome *c*, heme oxygenase 1 (HO-1), apoptosis-inducing factor (AIF), iNOS, phospho-p53 (pSer¹⁵), Bid, GAPDH, and goat anti-human PKCK2 antibodies were obtained from Santa Cruz Biotechnology (Santa Cruz, CA). Mouse polyclonal anti-human poly(ADP-ribose) polymerase (PARP) antibody was obtained from Oncogene (Cambridge, MA), and mouse monoclonal anti-human caspase 8 and phospho-p38 antibodies were from Cell Signaling Technology (Beverly, MA). Rabbit polyclonal anti-human Bid antibody (cleaved product), pSer antibody, and TUNEL reaction mixture were from Chemicon (Temecula, CA). Fluorescein isothiocyanate (FITC)-conjugated goat anti-rabbit IgG antibody and avidin-biotin-peroxidase (ABC) complex were obtained from Vector (Burlingame, CA), and Dulbecco's modified Eagle's medium (DMEM) and fetal bovine serum (FBS) were from Gibco (Gaithersburg, MD). Cilostazol (OPC-13013) was generously donated by Otsuka Pharmaceutical (Tokushima, Japan). Sodium nitroprusside (SNP) was obtained from Fluka (Buchs, Switzerland). DMSO, Hoechst 33342, RNase A, proteinase K, protease inhibitor cocktail, propidium iodide, 3,3'-diaminobenzidine (DAB), emodin, type II collagenase, mono-iodoacetate (MIA), and Safranin O were all obtained from Sigma (St. Louis, MO). The enhanced chemiluminescent Western blotting detection reagent (SuperSignal West Pico chemiluminescent substrate) was obtained from Pierce (Rockford, IL).

Cell culture of articular chondrocytes. Rat articular chondrocytes for primary culture were isolated from slices of knee joint cartilage from 5-week-old Sprague-Dawley rats. Chondrocytes were isolated by enzymatic digestion for 2 hours with 0.2% solid type II collagenase (381 units/mg) in DMEM. After collection of individual cells by brief centrifugation, cells were resuspended in DMEM supplemented with 10% (volume/volume) FBS, 50 μ g/ml of streptomycin, and 50 units/ml of penicillin. Cells were plated on culture dishes at a density of 5×10^4 cells/cm². Medium was replaced every 2 days, and cells reached confluence at ~5 days of culture. Cells from day-4 cultures were treated with the NO donor SNP. After incubation in the presence or absence of indicated pharmacologic reagents, such as cilostazol or emodin, for 24 hours, the cells were further exposed to 1.5 mM SNP for 24 hours.

Cell viability assay. Cell viability was determined with the Vi-Cell cell counter (Beckman Coulter, Fullerton, CA), which performs an automated trypan blue exclusion assay.

Nuclear morphology analysis of apoptosis. Twenty-four hours after SNP treatment, the cell suspension was cytospun onto a clean fat-free glass slide with a cytocentrifuge. Cytocentrifuged samples were fixed for 10 minutes in 4% paraformaldehyde and stained in 4 μ g/ml Hoechst 33342 for 30 minutes at 4°C. The total cell number (≥ 300 cells from each experiment) was counted using differential interference contrast (DIC) optics, and the number of cells showing condensed or fragmented nuclei on Hoechst staining was calculated using epifluorescence optics, by an observer who was blinded with regard to the experimental group.

DNA electrophoresis. Cells (2×10^6) were resuspended in 1.5 ml of lysis buffer (10 mM Tris [pH 7.5], 10 mM EDTA [pH 8.0], 10 mM NaCl, and 0.5% sodium dodecyl

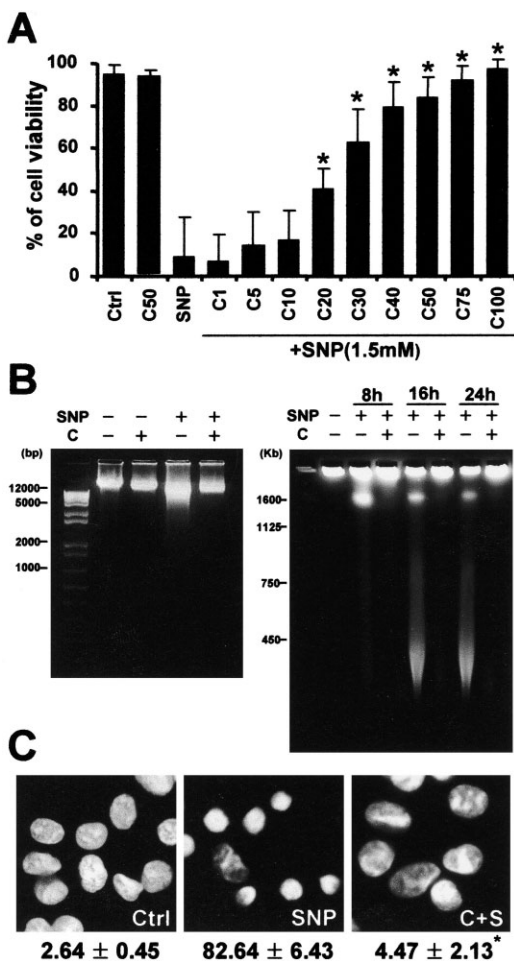


Figure 1. Prevention of sodium nitroprusside (SNP)-induced cell death in rat articular chondrocytes by cilostazol (C). **A**, Viability of cells pretreated with 1–100 μ M cilostazol 24 hours prior to treatment with 1.5 mM of the nitric donor SNP. Cells were harvested 24 hours after treatment with SNP, and viability was determined by automated trypan blue exclusion assay with a cell counter. Cilostazol pretreatment significantly prevented SNP-induced cell death in a dose-dependent manner, and with 50 μ M cilostazol, prevention of SNP-induced apoptosis was substantial. Bars show the mean and SD percent cell viability, as compared with untreated controls (Ctrl). * = $P < 0.05$ versus controls. **B**, Results of DNA electrophoresis (left) and pulsed-field gel electrophoresis (PFGE) (right) of cells left untreated, treated with 50 μ M cilostazol, treated with 1.5 mM SNP, or treated with both cilostazol and SNP. Conventional DNA electrophoresis of SNP-treated cells did not demonstrate ladder-like DNA fragments. PFGE of SNP-treated cells revealed the disintegration of nuclear DNA into giant fragments of 1–2 Mbp and high molecular weight fragments of 100–800 kbp, which was completely prevented by cilostazol treatment. **C**, Nuclear morphology of cells 24 hours after SNP treatment. Hoechst staining showed that cilostazol pretreatment significantly prevented SNP-induced nuclear condensation. C+S = cells treated with both cilostazol and SNP. Values are the mean \pm SD percentage of apoptotic cells with condensed nuclei. * = $P < 0.05$ versus controls.

sulfate [SDS]) to which proteinase K (200 μ g/ml) was added. After samples were incubated overnight at 48°C, 200 μ l of ice-cold 5M NaCl was added, and the supernatant containing fragmented DNA was collected after centrifugation. The DNA was then precipitated overnight at -20°C in 50% isopropanol and treated with RNase A for 1 hour at 37°C. A loading buffer containing 100 mM EDTA, 0.5% SDS, 40% sucrose, and 0.05% bromophenol blue was added at 1:5 (v/v). Separation was achieved in 2% agarose gels in Tris-acetic acid/EDTA buffer (containing 0.5 μ g/ml ethidium bromide) at 50 mA for 1.5 hours.

Pulsed-field gel electrophoresis (PFGE). Cells (2×10^6) were suspended in 50 μ l of phosphate buffered saline (PBS) containing 1% agarose with a low melting temperature. The cell suspension was poured into a template ($5 \times 2 \times 10$ mm), plugged, and cooled on ice. The hardened agarose gel blocks were incubated with 250 μ l of a mixture of proteinase K (1 mg/ml), *N*-lauroylsarcosine sodium (1% [weight/volume]), and 0.5M EDTA (pH 9.2) at 50°C for 48 hours. After incubation, half the volume of the digested agarose gel block was loaded into a sample well of a 1% (w/v) agarose gel (type II; $150 \times 150 \times 4.4$ mm) (Sigma) in $0.5 \times$ Tris-borate-EDTA (TBE) buffer (89 mM Tris-boric acid, 2 mM EDTA [pH 8.0]). PFGE was carried out in $0.5 \times$ TBE maintained at 14°C by circulating cool water for 16 hours (constant 6V; switch times initial 60 seconds and final 90 seconds), using the CHEF Mapper XA System (Bio-Rad, Hercules, CA). DNA in the gel was stained with ethidium bromide and detected with LAS-3000PLUS (Fuji Photo Film Company, Kanagawa, Japan). Chromosomal DNA from *Saccharomyces cerevisiae* (Bio-Rad, Hercules, CA) and a mixture of λ DNA, its concatemers, and *Hind* III-digested λ DNA (Sigma) were used as DNA size markers.

Subcellular fractionation. Cells (5×10^7) were washed in Tris-based, $\text{Mg}^{2+}/\text{Ca}^{2+}$ -deficient buffer (135 mM NaCl, 5 mM KCl, and 25 mM Tris Cl [pH 7.6]) and allowed to swell for 10 minutes in ice-cold hypotonic CaRSB buffer (10 mM NaCl, 1.5 mM CaCl_2 , 10 mM Tris HCl [pH 7.5], and $1 \times$ protease inhibitor cocktail). Cells were dounced with 60 strokes, and mitochondria stabilization buffer (210 mM mannitol, 70 mM sucrose, 5 mM EDTA, and 5 mM Tris [pH 7.6]) was added to stabilize mitochondria (2 ml of $2.5 \times$ per 3 ml of homogenate). After collecting the nucleus (by centrifuging twice at 3,000 revolutions per minute for 15 minutes), the supernatant was spun at 14,000 rpm for 20 minutes at 4°C. The pellet and the supernatant included mitochondria and cytoplasm, respectively.

Western blot analysis. Cells (2×10^6) were washed twice in ice-cold PBS, resuspended in 200 μ l ice-cold solubilizing buffer (300 mM NaCl, 50 mM Tris Cl [pH 7.6], 0.5% Triton X-100, 2 mM phenylmethylsulfonyl fluoride [PMSF], 2 μ l/ml aprotinin, and 2 μ l/ml leupeptin) and incubated at 4°C for 30 minutes. The lysates were centrifuged at 14,000 rpm for 20 minutes at 4°C. Protein concentrations of cell lysates were determined with Bradford protein assay reagent (Bio-Rad, Richmond, CA) and 40 μ g of proteins was loaded onto 7.5–15% SDS-polyacrylamide gels. The gels were transferred to nitrocellulose membranes (Amersham Pharmacia Biotech, Piscataway, NJ) and reacted with each antibody. Immunostaining with antibodies was performed using SuperSignal West

Pico enhanced chemiluminescent substrate and detected with LAS-3000PLUS.

Coimmunoprecipitation. Cells were collected and lysed in 1 ml of immunoprecipitation lysis buffer (300 mM NaCl, 500 mM Tris Cl [pH 7.6], 0.5% Triton X-100, protease inhibitors, 10 mM $\text{Na}_4\text{P}_2\text{O}_7$, 1 mM Na_3VO_4 , 25 mM NaF, and 1mM β -glycerophosphate). Protein concentrations of cell lysates were determined using the Bradford method, and 500 μg of protein was precleared and then incubated with anti-phosphorylated serine antibody in extraction buffer at 4°C overnight. The immune complexes were precipitated with protein A/G-agarose beads (Santa Cruz Biotechnology) for 2 hours, and washed 5 times with extraction buffer prior to boiling in SDS sample buffer. Immunoprecipitated proteins were separated by SDS-polyacrylamide gel electrophoresis, and Western blot analysis was performed as described above.

Immunofluorescence staining and confocal microscopy. A cell suspension was cytospun onto a clean fat-free glass slide with a cytocentrifuge. Cells were incubated with anti-cytochrome *c*, AIF, and Bid antibodies for 1 hour, washed 3 times for 5 minutes each, and then incubated with FITC-conjugated secondary antibody for 1 hour at room temperature. Fluorescent images were observed and analyzed under a Zeiss LSM 510 confocal laser scanning microscope (Zeiss, Gottingen, Germany).

PKCK2 activity assay. PKCK2 activity was measured using a casein kinase 2 assay kit (Upstate Biotechnology, Lake Placid, NY). A recombinant full-length human PKCK2 protein that contains an α -subunit N-terminal 6 \times His-Tag and a β -subunit N-terminal genome signature tag (Upstate Biotechnology) was used as a positive control.

Rat model of OA. *Animals.* Fifteen Sprague-Dawley rats weighing 175–200 gm were used. The study was approved by the ethics committee of Dong-A University and fulfilled the guidelines for animal experiments established by The Korean Academy of Medical Sciences. OA was induced in 5 rats by intraarticular injection of MIA, as described previously (12). Briefly, 1 mg of MIA in 0.1 ml of physiologic saline solution was injected once a week for 4 weeks into the right knees. Cilostazol (30 mg/kg/day) was administered orally once daily beginning the day after the first injection of MIA. Five additional rats received MIA alone, and 5 rats received no MIA or cilostazol and were used as controls.

Tissue preparation and histologic examination. At the end of the 4 weeks, animals were killed by ether inhalation. Both knee joints from each animal were dissected, and femoral condyles were fixed in PBS (pH 7.4) containing 4% paraformaldehyde, decalcified in 12.5% EDTA, dehydrated, and embedded in paraffin blocks. Five-micrometer microsections were prepared and stained with hematoxylin and eosin and with Safranin O.

TUNEL staining. Sections were incubated with proteinase K (20 $\mu\text{g}/\text{ml}$) for 15 minutes at room temperature, in 2% H_2O_2 solution for 5 minutes at room temperature, and then with terminal deoxynucleotidyl transferase (TdT) enzyme for 1 hour at 37°C. Next, antidigoxigenin-peroxidase was applied to the sections for 30 minutes at room temperature and developed with 0.05% DAB. Staining for the negative control was undertaken by skipping the TdT application. Sections were observed and photographed under DIC optics without any counterstaining.

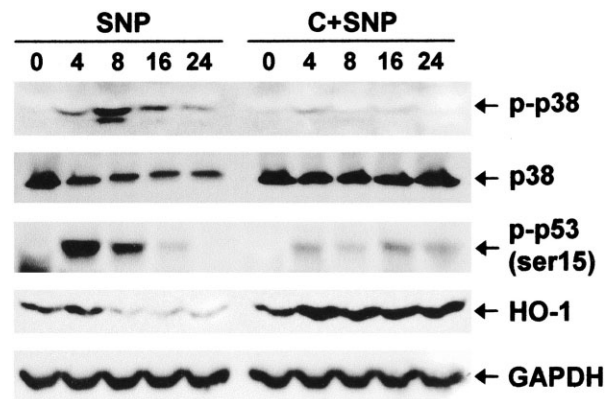


Figure 2. Prevention of SNP-induced down-regulation of heme oxygenase 1 (HO-1) and up-regulation of phosphorylated p38 and phosphorylated p53 by 50 μM cilostazol. Western blots of antibodies to anti-phosphorylated p38, anti-phosphorylated p53 (Ser¹⁵), and anti-HO-1, before pretreatment (0) and 4, 8, 16, and 24 hours after treatment with SNP alone or with SNP and cilostazol, are shown; p38 was used as the loading control for phosphorylated p38. Cilostazol pretreatment prevented SNP-induced down-regulation of HO-1 as well as SNP-induced up-regulation of phosphorylated p38 and phosphorylated p53. GAPDH was used as a loading control. See Figure 1 for other definitions.

Immunohistochemistry. Sections were incubated in goat serum solution (diluted 1:70) for 30 minutes at room temperature, and then with primary antibody (diluted 1:100) for 2 hours at room temperature. Next, sections were incubated with secondary antibody for 1 hour at 37°C and developed using ABC complex, and peroxidase was revealed by DAB.

Statistical analysis. Four independent experiments were carried out in vitro. Results are expressed as the mean \pm SD from 4 experiments performed in triplicate.

RESULTS

Prevention of NO-induced apoptosis in rat articular chondrocytes by cilostazol. Cilostazol prevented NO-induced cell death in a dose-dependent manner (Figure 1A). Since cilostazol substantially prevented NO-induced cell death at 50 μM , this concentration was used for further exploration of the mechanism of preventing cell death. Various assays were performed in order to confirm that cilostazol prevented NO-induced cell death by blocking apoptosis. Although cells treated with the NO donor SNP failed to show ladder-like DNA fragments from their genomic DNA on agarose gel, PFGE revealed the disintegration of nuclear DNA into giant fragments of 1–2 Mbp and high molecular weight fragments of 100–800 kbp. Cilostazol appeared to completely prevent these giant and high molecular weight fragmentations (Figure 1B). We also observed that

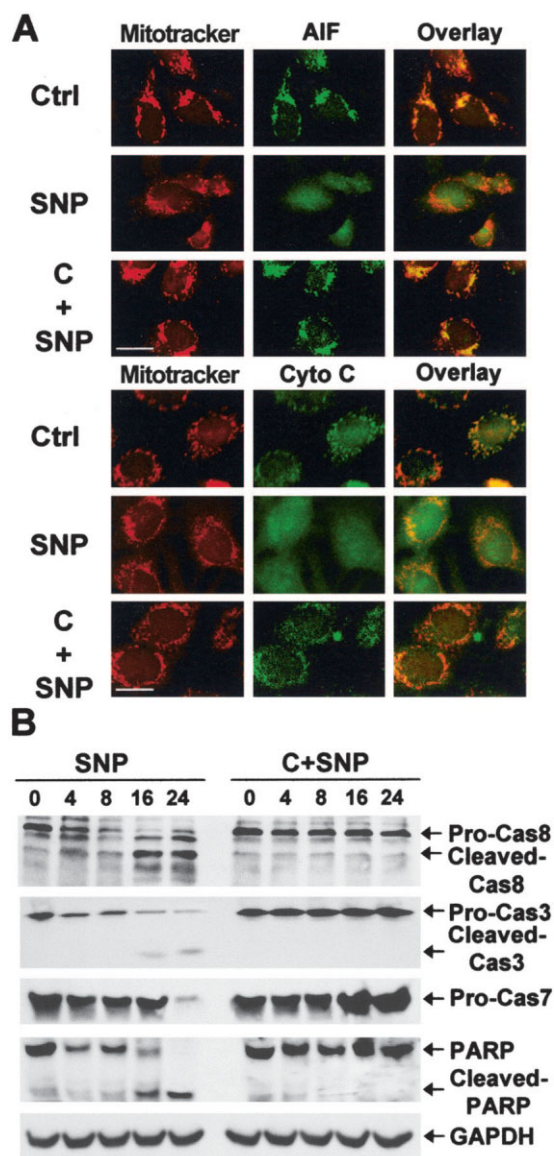


Figure 3. Prevention of the release of mitochondrial apoptotic factors and the activation of caspases by 50 μ M cilostazol. **A**, Confocal microscopy images showing localization of Mitotracker stains, apoptosis-inducing factor (AIF), and cytochrome *c* (Cyto *c*) on the mitochondria in control cells, and release of both AIF and cytochrome *c* from mitochondria by SNP treatment. Cilostazol pretreatment prevented SNP-induced release of AIF and cytochrome *c* from mitochondria. Bars = 20 μ m. **B**, Western blots of caspase 8 (pro-Cas8), caspase 3 (pro-Cas3), caspase 7 (pro-Cas7), and poly(ADP-ribose) polymerase (PARP), before pretreatment (0) and 4, 8, 16, and 24 hours after treatment with SNP alone or with SNP and cilostazol. Cilostazol pretreatment prevented SNP-induced degradation of caspase 8, caspase 3, and caspase 7 and SNP-induced production of caspase 8 and caspase 3 cleaved products. Cilostazol pretreatment also prevented the degradation of the caspase substrate PARP and its cleavage by SNP. GAPDH was used as a loading control. See Figure 1 for other definitions.

cilostazol prevented NO-induced nuclear condensation (Figure 1C). These findings support the notion that cilostazol protects cells against NO-induced apoptosis.

Prevention of NO-induced down-regulation of HO-1 and of up-regulation of phosphorylated p38 and p53 by cilostazol. Activation of p38 and resultant phosphorylation of p53 is crucial in NO-induced cell death of cultured articular chondrocytes (32). Thus, we examined whether the prevention of cell death by cilostazol was mediated via these factors. Our results showed that cilostazol prevented NO-induced up-regulation of phosphorylated p38 and p53. Since HO-1, a cytoprotective factor, is also known to be involved in NO-induced chondrocyte injury (33), we next examined whether cilostazol modulates the expression of HO-1 in chondrocytes treated with SNP. We found that cilostazol prevented NO-induced down-regulation of HO-1 (Figure 2).

Prevention of the release of mitochondrial apoptotic factors and of the activation of caspases by cilostazol. NO-induced apoptosis has been demonstrated to be accompanied by the opening of mitochondrial permeability transition pores and by the release of AIF and cytochrome *c* from mitochondria (34,35). Therefore, we examined whether cilostazol prevented these mitochondrial events. Our results showed that NO induced the release of AIF and cytochrome *c* from mitochondria in rat chondrocytes, and that cilostazol prevented the release of these factors from mitochondria (Figure 3A). Caspases play an essential role in most types of apoptosis, including NO-induced apoptosis. We found that caspase 3 and caspase 7 were activated in NO-induced apoptosis and that cilostazol prevented the activation of these effector caspases. In addition, the processing of initiator caspase 8 was observed in NO-induced apoptosis, and this was also inhibited by cilostazol. Cilostazol also prevented SNP-mediated cleavage of a caspase substrate, PARP (Figure 3B).

Cilostazol causes phosphorylated Bid to accumulate in both the nucleus and cytosol and prevents NO-induced down-regulation of PKCK2 expression and reduction of PKCK2 activity. It is well known that Bid plays an essential role in caspase 8-mediated apoptosis. Thus, we next examined whether cilostazol prevents NO-induced apoptosis by modulating Bid. Western blotting using the antibody detecting cleaved Bid demonstrated that SNP induced mitochondrial translocation of cleaved Bid (Figure 4A). Confocal microscopy also showed that SNP induced mitochondrial translocation of Bid (Figure 4B). In addition, coimmunoprecipitation showed that SNP downregulated phosphorylated Bid in the nucleus and cytosol (Figure 4C). Notably, cilostazol

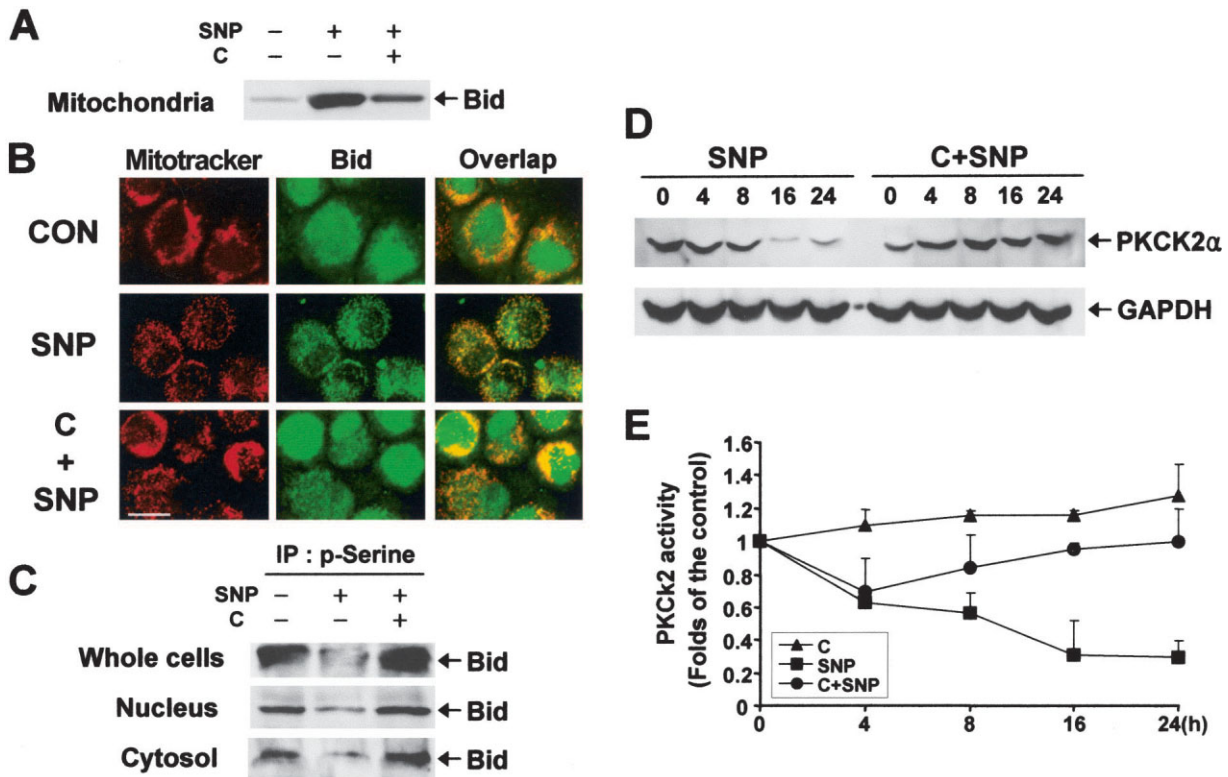


Figure 4. Accumulation of phosphorylated Bid in both the nucleus and cytosol and prevention of SNP-induced down-regulation of protein kinase CK2 (PKCK2) expression and decrease of PKCK2 activity by 50 μ M cilostazol. **A**, Western blot showing SNP-induced mitochondrial translocation of cleaved Bid, which was prevented by cilostazol pretreatment. **B**, Confocal microscopy images showing localization of Bid in the nucleus or cytosol in control (CON) cells, and translocation of Bid onto mitochondria as a result of SNP treatment. Cilostazol pretreatment prevented SNP-induced mitochondrial translocation of Bid. Bar = 20 μ m. **C**, Coimmunoprecipitation assay showing that cilostazol pretreatment prevented SNP-induced down-regulation of phosphorylated Bid in the nucleus and cytosol. IP = immunoprecipitation. **D**, Western blot of PKCK2 α , before pretreatment (0), and 4, 8, 16, and 24 hours after treatment with SNP alone or with cilostazol and SNP. Cilostazol pretreatment prevented SNP-induced down-regulation of PKCK2. GAPDH was used as a loading control. **E**, Results of a PKCK2 activity assay, showing that cilostazol pretreatment prevented SNP-induced reduction in PKCK2 activity. Values are the mean and SD. See Figure 1 for other definitions.

prevented not only the mitochondrial translocation of Bid but also the down-regulation of phosphorylated Bid in the nucleus and cytosol (Figures 4A–C).

We next tested whether the protection of cells against NO-induced apoptosis by cilostazol was mediated via PKCK2. Western blot analysis revealed that the expression level of PKCK2 catalytic subunit α was reduced after SNP treatment (Figure 4D). In addition, SNP treatment resulted in a decrease in PKCK2 activity (Figure 4E). Importantly, cilostazol prevented not only NO-induced down-regulation of PKCK2 but also the NO-induced reduction of PKCK2 activity (Figures 4D and E).

Prevention of NO-induced apoptosis by cilostazol through PKCK2. To corroborate that cilostazol-mediated prevention of NO-induced apoptosis occurs via PKCK2, we performed several assays using a PKCK2

inhibitor, emodin (36). A cell viability assay showed that 50 μ M emodin counteracted the effect of cilostazol on NO-induced chondrocyte death (Figure 5A). Western blot analysis also showed that 50 μ M emodin abolished the ability of cilostazol to prevent NO-induced down-regulation of Bid (Figure 5B). Emodin also abolished the ability of cilostazol to prevent NO-induced mitochondrial translocation of cleaved Bid (Figure 5C). Furthermore, it abolished the ability of cilostazol to prevent NO-induced down-regulation of phosphorylated Bid in cytosol (Figure 5D). An assay for PKCK2 activity showed that emodin abolished the ability of cilostazol to prevent NO-induced reduction of PKCK2 activity (Figure 5E).

Prevention of cartilage destruction and of chondrocyte apoptosis by cilostazol in rats with MIA-induced OA. Cartilage obtained from rats injected with MIA showed

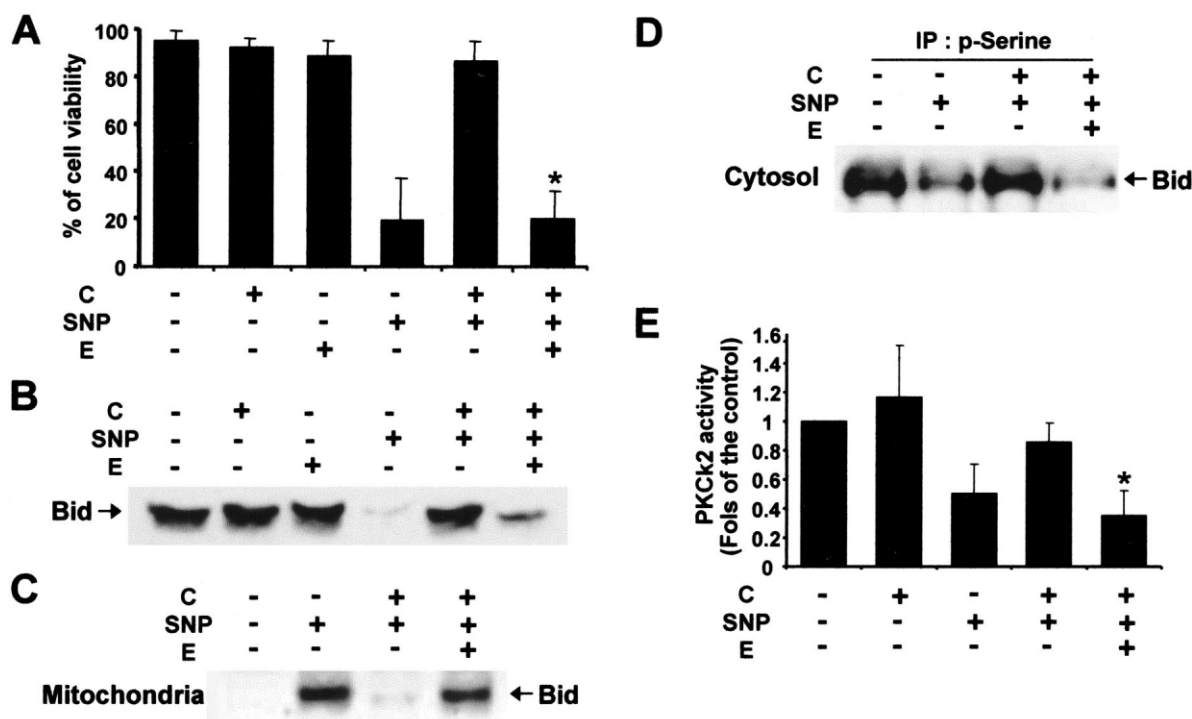


Figure 5. Prevention of SNP-induced apoptosis by cilostazol via protein kinase CK2 (PKCK2). After simultaneous pretreatment with 50 μ M emodin (E) and 50 μ M cilostazol for 24 hours, cells were further exposed to 1.5 mM SNP for 24 hours. **A**, Cell viability, determined by automated trypan blue exclusion assay with a cell counter. Emodin significantly abolished the ability of cilostazol to prevent SNP-induced chondrocyte death. Bars show the mean and SD percent cell viability, as compared with untreated controls. * = $P < 0.05$ versus controls. **B**, Western blot showing that emodin abolished the ability of cilostazol to prevent SNP-induced down-regulation of Bid expression. **C**, Western blot showing that emodin abolished the ability of cilostazol to prevent SNP-induced mitochondrial translocation of cleaved Bid. **D**, Coimmunoprecipitation showing that emodin abolished the ability of cilostazol to prevent SNP-induced down-regulation of phosphorylated Bid in cytosol. IP = immunoprecipitation. **E**, Results of a PKCK2 activity assay, showing that emodin significantly abolished the ability of cilostazol to prevent SNP-induced reduction in PKCK2 activity. Bars show the mean and SD. * = $P < 0.05$ versus untreated cells. See Figure 1 for other definitions.

structural changes, including changes characteristic of OA, such as irregular surfaces, the disappearance of surface-layer cells, slightly diffuse cell growth in the transitional and radial zones, and slightly reduced Safranin O staining. Most chondrocytes displayed a positive TUNEL reaction. Cilostazol prevented this MIA-induced cartilage degeneration. A previous study showed that iNOS was expressed in the early stages of experimental OA (37). Consistent with those results, our immunohistochemical analysis also showed that iNOS was expressed in most chondrocytes. Notably, cilostazol reduced the level of expression of iNOS (Figure 6).

DISCUSSION

The results of this study support the hypothesis that PKCK2 is involved in NO-induced apoptosis of rat articular chondrocytes and that cilostazol protects rat

chondrocytes against NO-induced apoptosis via PKCK2 in vitro. Furthermore, our findings support the notion that cilostazol prevents cartilage destruction in MIA-induced OA in a rat model in which iNOS is expressed.

The recent observation that cilostazol inhibits apoptosis under several circumstances (12,20–22) raises the interesting possibility that it can be considered as a therapy for diseases associated with excess apoptosis. Although apoptotic chondrocyte death is not always a widespread phenomenon in cartilage aging or OA cartilage degeneration (38), obviously any kind of cell death is detrimental to the tissue. Therefore, any strategy to prevent chondrocyte death or to manipulate the mechanism mediated by stimuli that cause cell death has potential for substantial therapeutic impact (39).

Although understanding of the mechanism by which cilostazol protects cells against apoptosis remains

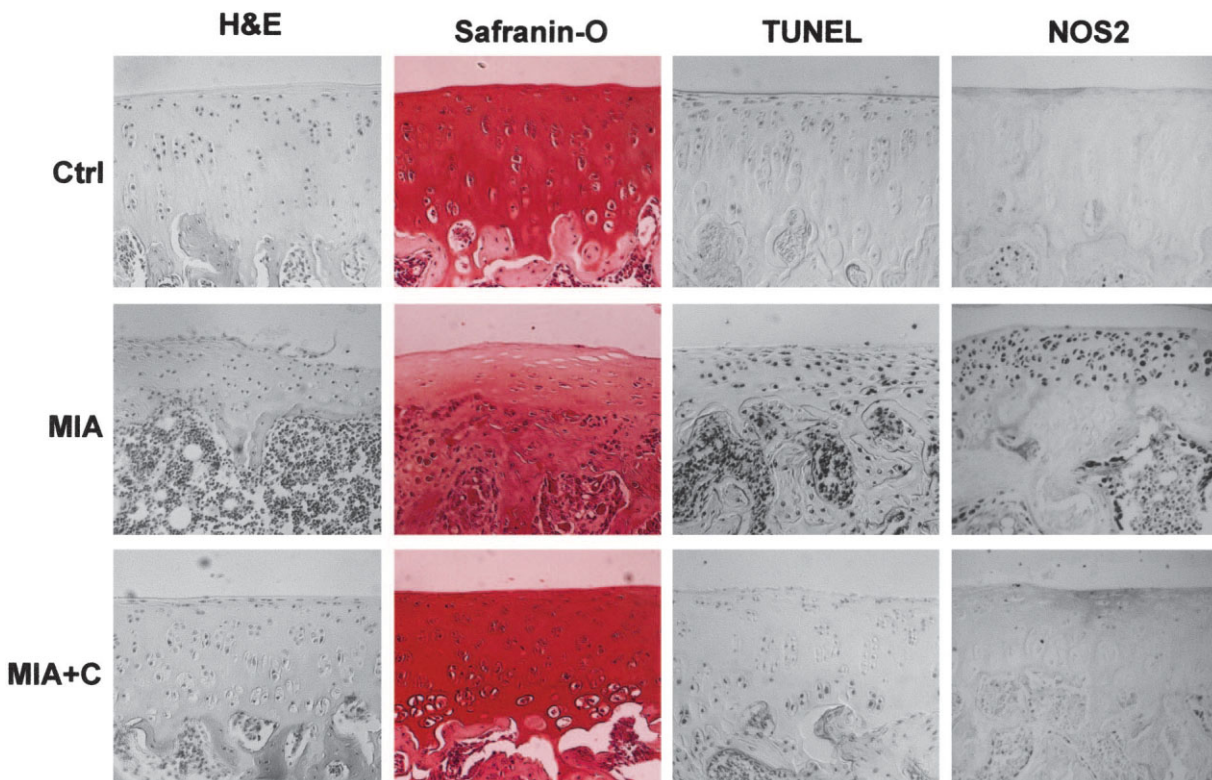


Figure 6. Prevention of cartilage destruction and chondrocyte apoptosis by cilostazol in rats with mono-iodoacetate (MIA)-induced osteoarthritis. Hematoxylin and eosin (H&E) staining showed that cilostazol prevented MIA-induced cartilage surface irregularity and slightly diffuse cell growth in the transitional and radial zones. Cilostazol also prevented MIA-induced reduction of Safranin O staining and increased expression of TUNEL-positive chondrocytes. Immunohistochemical analysis showed that cilostazol prevented MIA-induced expression of inducible nitric oxide synthase (iNOS [NOS2]). See Figure 1 for other definitions.

far from complete, recent evidence has yielded certain insights. Previous studies (20,21) have shown that cilostazol reverses decreases in Bcl-2 protein and increases in Bax protein production and cytochrome *c* release. The maxi-K channel opening-coupled up-regulation and down-regulation of PTEN phosphorylation with resultant increases in Akt and CREB phosphorylation and increased Bcl-2 protein levels have also been demonstrated (12). In addition, suppression of NAD(P)H oxidase-dependent superoxide formation and of cytokine induction has been demonstrated (22). In a few apoptosis systems showing the prevention of apoptosis by cilostazol, PKCK2 has also been reported to play a crucial role (12,23).

PKCK2 is a constitutively active, growth factor-independent serine/threonine protein kinase (40) composed of 2 catalytic α (and/or α') subunits and 2 regulatory β subunits (41). Although it is well known that PKCK2 participates in various cellular functions, its biologic activity on chondrocytes has not been previously

described. In the present study, we demonstrated the presence of PKCK2 activity on rat articular chondrocytes.

We also demonstrated that PKCK2 is involved in the regulation of rat articular chondrocyte apoptosis. It has been well documented that PKCK2 is involved in the regulation of apoptosis by phosphorylating some apoptosis-related factors. PKCK2 activity has been found to be consistently enhanced in various tumor cells (42–44), and increased expression of PKCK2 has protected cells against Fas- and drug-induced apoptosis (45,46). Furthermore, inhibitors of PKCK2 have been reported to trigger apoptosis and increase the susceptibility of cancer cells to chemotherapeutic agents or apoptotic stimuli (47–49). Thus, PKCK2 appears to have a general antiapoptotic function.

Through recent studies, advances have been made in understanding the mechanism by which PKCK2 supports cell survival. Phosphorylation of Max, the transcription partner of the *c-Myc* protooncogene, by

PKCK2 protected it against caspase-mediated cleavage (50). It has also been demonstrated that phosphorylation by PKCK2 is required for the apoptotic protein ARC to exert its inhibitory activity on caspase 8 (30) and that PKCK2-regulated procaspase 2 activation plays a central role in both death receptor-mediated and stress-mediated apoptosis (31). Furthermore, overexpression of PKCK2 blocked the mitochondrial apoptosis machinery engaged by TRAIL (51). Thus, further determination of the exact molecular mechanisms through which PKCK2 modulates apoptosis of chondrocytes could lead to better prevention and treatment of OA.

This study showed that cilostazol prevented NO-induced apoptosis in articular chondrocytes by modulating signaling events, such as activation of p38, phosphorylation of p53, and down-regulation of HO-1, and mitochondrial events, such as the release of cytochrome *c* and AIF. We also demonstrated that cilostazol prevented the degradation of Bid and its mitochondrial translocation, and caused phosphorylated Bid to accumulate in the nucleus and cytosol.

Bid, which is the best-characterized connection between the intrinsic and extrinsic apoptosis pathways, translocates to mitochondria after cleavage by caspase 8, causing proapoptotic changes. Previous studies have shown that Bid was processed by caspases in NO-induced apoptosis (21,52). However, the molecular role of Bid in NO-induced apoptosis has not been fully delineated. This is the first report to describe the role of Bid in NO-induced apoptosis of chondrocytes. Our findings, which showed that the apoptosis-preventing effect of cilostazol resulted at least in part from modulation of Bid, raise another important point regarding the efficacy of cilostazol. According to the findings of previous studies, PKCK2 regulates Bid activity, and Bid phosphorylated by PKCKs is insensitive to caspase cleavage (45,47,53). We therefore conclude that cilostazol phosphorylates Bid by modulating PKCK2 expression and activity, which confers the resistance of Bid to caspase cleavage, resulting in the prevention of NO-induced apoptosis.

Although findings in rats with MIA-induced experimental OA cannot be translated to human OA, as indicated by a recent study showing that there is little transcriptional similarity between iodoacetate-induced arthritis in rats and human OA-derived cartilage (54), experimental models have often been used for new target discovery/validation and drug evaluation in OA. MIA is known to disturb chondrocyte metabolism and to induce iNOS, resulting in induction of chondrocyte apoptosis and loss of cartilage matrix. The present study

showed that cilostazol prevented apoptosis of articular chondrocytes and destruction of cartilage in MIA-induced OA in rats. Furthermore, we observed that cilostazol prevented the induction of iNOS. Thus, we propose that cilostazol inhibits iNOS expression in chondrocytes in an experimental model of OA, leading to the prevention of chondrocyte apoptosis and cartilage destruction, although we did not examine antiinflammatory action and inhibitory effects of cilostazol on MMPs.

Taken together, our findings show that cilostazol protects rat chondrocytes against NO-induced apoptosis via PKCK2 in vitro and prevents cartilage destruction in a rat model of OA. Further studies are needed to determine the exact mechanism of action of cilostazol.

AUTHOR CONTRIBUTIONS

Dr. Yoo had full access to all of the data in the study and takes responsibility for the integrity of the data and the accuracy of the data analysis.

Study design. Sung Won Lee, Yoo.

Acquisition of data. Song, Shin, Kyung Taek Kim, Kunhong Kim, Sang Yeob Lee, Chung.

Analysis and interpretation of data. Young Chul Park.

Manuscript preparation. Bong Soo Park, Yun, Hye Jeong Lee.

Statistical analysis. Song.

REFERENCES

1. Mankin HJ, Dorfman H, Lippiello L, Zarins A. Biochemical and metabolic abnormalities in articular cartilage from osteoarthritic human hips. II. Correlation of morphology with biochemical and metabolic data. *J Bone Joint Surg Am* 1971;53:523–37.
2. Hashimoto S, Ochs RL, Komiya S, Lotz M. Linkage of chondrocyte apoptosis and cartilage degradation in human osteoarthritis. *Arthritis Rheum* 1998;41:1632–8.
3. Kim HA, Lee YJ, Seong SC, Choe KW, Song YW. Apoptotic chondrocyte death in human osteoarthritis. *J Rheumatol* 2000;27:455–62.
4. Hashimoto S, Takahashi K, Amiel D, Coutts RD, Lotz M. Chondrocyte apoptosis and nitric oxide production during experimentally induced osteoarthritis. *Arthritis Rheum* 1998;41:1266–74.
5. Blanco FJ, Ochs RL, Schwarz H, Lotz M. Chondrocyte apoptosis induced by nitric oxide. *Am J Pathol* 1995;146:75–85.
6. Amin AR, Abramson SB. The role of nitric oxide in articular cartilage breakdown in osteoarthritis. *Curr Opin Rheumatol* 1998;10:263–8.
7. Kim SJ, Ju JW, Oh CD, Yoon YM, Song WK, Kim JH, et al. ERK-1/2 and p38 kinase oppositely regulate nitric oxide-induced apoptosis of chondrocytes in association with p53, caspase-3, and differentiation status. *J Biol Chem* 2002;277:1332–9.
8. Miwa M, Saura R, Hirata S, Hayashi Y, Mizuno K, Itoh H. Induction of apoptosis in bovine articular chondrocyte by prostaglandin E₂ through cAMP-dependent pathway. *Osteoarthritis Cartilage* 2000;8:17–24.
9. Hashimoto S, Setareh M, Ochs RL, Lotz M. Fas/Fas ligand expression and induction of apoptosis in chondrocytes. *Arthritis Rheum* 1997;40:1749–55.

10. Kuhn K, Lotz M. Regulation of CD95 (Fas/APO-1)-induced apoptosis in human chondrocytes. *Arthritis Rheum* 2001;44:1644–53.
11. Aizawa T, Kon T, Einhorn TA, Gerstenfeld LC. Induction of apoptosis in chondrocytes by tumor necrosis factor- α . *J Orthop Res* 2001;19:785–96.
12. Lee SW, Lee HJ, Chung WT, Choi SM, Rhyu SH, Kim DK, et al. TRAIL induces apoptosis of chondrocytes and influences the pathogenesis of experimentally induced rat osteoarthritis. *Arthritis Rheum* 2004;50:534–42.
13. Cao M, Westerhausen-Larson A, Niyibizi C, Kavalkovich K, Georgescu HI, Rizzo CF, et al. Nitric oxide inhibits the synthesis of type-II collagen without altering Col2A1 mRNA abundance: prolyl hydroxylase as a possible target. *Biochem J* 1997;324:305–10.
14. Notoya K, Jovanovic DV, Reboul P, Martel-Pelletier J, Mineau F, Pelletier JP. The induction of cell death in human osteoarthritis chondrocytes by nitric oxide is related to the production of prostaglandin E₂ via the induction of cyclooxygenase-2. *J Immunol* 2000;165:3402–10.
15. Kimura Y, Tani T, Kanbe T, Watanabe K. Effect of cilostazol on platelet aggregation and experimental thrombosis. *Arzneimittelforschung* 1985;35:1144–9.
16. Tanaka K, Gotoh F, Fukuuchi A, Amano T, Uematsu D, Kawamura J, et al. Effects of a selective inhibitor of cyclic AMP phosphodiesterase on the pial microcirculation in feline cerebral ischemia. *Stroke* 1989;20:668–73.
17. Jaff MR. Pharmacotherapy for peripheral arterial disease: emerging therapeutic options. *Angiology* 2002;53:627–33.
18. Dawson DL, Cutler BS, Meissner MH, Strandness DE Jr. Cilostazol has beneficial effects in treatment of intermittent claudication: result from a multicenter, randomized, prospective, double-blind trial. *Circulation* 1998;98:678–86.
19. Tsai CS, Lin FY, Chen YH, Yang TL, Wang HJ, Huang GS, et al. Cilostazol attenuates MCP-1 and MMP-9 expression in vivo in LPS-administrated balloon-injured rabbit aorta and in vitro in LPS-treated monocytic THP-1 cells. *J Cell Biochem* 2007. E-pub ahead of print.
20. Kim KY, Shin HK, Choi JM, Hong KW. Inhibition of lipopolysaccharide-induced apoptosis by cilostazol in human umbilical vein endothelial cells. *J Pharmacol Exp Ther* 2002;300:709–15.
21. Choi JM, Shin HK, Kim KY, Lee JH, Hong KW. Neuroprotective effect of cilostazol against focal cerebral ischemia via antiapoptotic action in rats. *J Pharmacol Exp Ther* 2000;300:787–93.
22. Shin HK, Kim YK, Kim KY, Lee JH, Hong KW. Remnant lipoprotein particles induce apoptosis in endothelial cells by NAD(P)H oxidase-mediated production of superoxide and cytokines via lectin-like oxidized low-density lipoprotein receptor-1 activation: prevention by cilostazol. *Circulation* 2004;109:1022–8.
23. Kim KY, Shin HK, Lee JH, Kim CD, Lee WS, Rhim BY, et al. Cilostazol enhances casein kinase 2 phosphorylation and suppresses tumor necrosis factor- α -induced increased phosphatase and tensin homolog deleted from chromosome 10 phosphorylation and apoptotic cell death in SK-N-SH cells. *J Pharmacol Exp Ther* 2004;308:97–104.
24. Hanks SK, Hunter T. Protein kinases 6. The eukaryotic protein kinase superfamily: kinase (catalytic) domain structure and classification. *FASEB J* 1995;9:576–96.
25. Hunter T, Plowman GD. The protein kinases of budding yeast: six scores and more. *Trends Biochem Sci* 1997;22:18–22.
26. Allende JE, Allende CC. Protein kinases. 4. Protein kinase CK2: an enzyme with multiple substrates and a puzzling regulation. *FASEB J* 1995;9:313–23.
27. Luscher B, Kuenzel EA, Krebs EG, Eisenman RN. Myc oncoproteins are phosphorylated by casein kinase II. *EMBO J* 1989;2:1111–9.
28. McElhinny JA, Trushin SA, Bren GD, Chester N, Paya CV. Casein kinase II phosphorylates I κ B α at S-283, S-289, S-293, and T-291 and is required for its degradation. *Mol Cell Biol* 1996;16:899–906.
29. Keller DM, Zeng X, Wang Y, Zhang QH, Kapoor M, Shu H, et al. A DNA damage-induced p53 serine 392 kinase complex contains CK2, hSpt16, and SSRP1. *Mol Cell* 2001;7:283–92.
30. Li PF, Li J, Muller EC, Otto A, Dietz R, von Harsdorf R. Phosphorylation by protein kinase CK2: a signaling switch for the caspase-inhibiting protein ARC. *Mol Cell* 2002;10:247–58.
31. Shin S, Lee Y, Kim W, Ko H, Choi H, Kim K. Caspase-2 primes cancer cells for TRAIL-mediated apoptosis by processing procaspase-8. *EMBO J* 2005;24:3532–42.
32. Kim SJ, Hwang SG, Shin DY, Kang SS, Chun JS. p38 kinase regulates nitric oxide-induced apoptosis of articular chondrocytes by accumulating p53 via NF κ B-dependent transcription and stabilization by serine 15 phosphorylation. *J Biol Chem* 2002;277:33501–8.
33. Fernandez P, Guillen MI, Gomar F, Alcaraz MJ. Expression of heme oxygenase-1 and regulation by cytokines in human osteoarthritic chondrocytes. *Biochem Pharmacol* 2003;66:2049–52.
34. Jin HO, Park IC, An S, Lee HC, Woo SH, Hong YJ, et al. Up-regulation of Bak and Bim via JNK downstream pathway in the response to nitric oxide in human glioblastoma cells. *J Cell Physiol* 2006;206:477–86.
35. Moriya R, Uehara T, Nomura Y. Mechanism of nitric oxide-induced apoptosis in human neuroblastoma SH-SY5Y cells. *FEBS Lett* 2000;484:253–60.
36. Yim H, Lee YH, Lee CH, Lee SK. Emodin, an anthraquinone derivative isolated from the rhizomes of *Rheum palmatum*, selectively inhibits the activity of casein kinase II as a competitive inhibitor. *Planta Med* 1999;65:9–13.
37. Dumond H, Presle N, Pottier P, Pacquelet S, Terlain B, Netter P, et al. Site specific changes in gene expression and cartilage metabolism during early experimental osteoarthritis. *Osteoarthritis Cartilage* 2004;12:284–95.
38. Aigner T, Hemmel M, Neureiter D, Gebhard PM, Zeiler G, Kirchner T, et al. Apoptotic cell death is not a widespread phenomenon in normal aging and osteoarthritic human articular knee cartilage: a study of proliferation, programmed cell death (apoptosis), and viability of chondrocytes in normal and osteoarthritic human knee cartilage. *Arthritis Rheum* 2001;44:1304–12.
39. Aigner T, Haag J, Martin J, Buckwalter J. Osteoarthritis: aging of matrix and cells—going for a remedy. *Curr Drug Targets* 2007;8:325–31.
40. Litchfield DW, Dobrowolska G, Krebs EG. Regulation of casein kinase II by growth factors: a reevaluation. *Cell Mol Biol Res* 1994;40:373–81.
41. Xu X, Toselli PA, Russell LD, Seldin DC. Globozoospermia in mice lacking the casein kinase II α' catalytic subunit. *Nat Genet* 1999;23:118–21.
42. Munstermann U, Fritz G, Seitz G, Lu YP, Schneider HR, Issinger OG. Casein kinase II is elevated in solid human tumours and rapidly proliferating non-neoplastic tissue. *Eur J Biochem* 1990;189:251–7.
43. Landesman-Bollag E, Romieu-Mourez R, Song DH, Sonenshein GE, Cardiff RD, Seldin DC. Protein kinase CK2 in mammary gland tumorigenesis. *Oncogene* 2001;20:3247–57.
44. Faust RA, Niehans G, Gapany M, Hoistad D, Knapp D, Cherwitz D, et al. Subcellular immunolocalization of protein kinase CK2 in normal and carcinoma cells. *Int J Biochem Cell Biol* 1999;31:941–9.
45. Desagher S, Osen-Sand A, Montessuit S, Magnenat E, Vilbois F, Hochmann A, et al. Phosphorylation of bid by casein kinases I and II regulates its cleavage by caspase 8. *Mol Cell* 2001;8:601–11.
46. Guo C, Yu S, Davis AT, Wang H, Green JE, Ahmed K. A potential role of nuclear matrix-associated protein kinase CK2 in

- protection against drug-induced apoptosis in cancer cells. *J Biol Chem* 2001;276:5992–9.
47. Ruzzene M, Penzo D, Pinna LA. Protein kinase CK2 inhibitor 4, 5, 6, 7-tetrabromobenzotriazole (TBB) induces apoptosis and caspase-dependent degradation of haematopoietic lineage cell-specific protein 1 (HS1) in Jurkat cells. *Biochem J* 2002;364:41–7.
 48. Ravi R, Bedi A. Sensitization of tumor cells to Apo2 ligand/TRAIL-induced apoptosis by inhibition of casein kinase II. *Cancer Res* 2002;62:4180–5.
 49. Faust RA, Tawfic S, Davis AT, Bubash LA, Ahmed K. Antisense oligonucleotides against protein kinase CK2- α inhibit growth of squamous cell carcinoma of the head and neck in vitro. *Head Neck* 2000;22:341–6.
 50. Krippner-Heidenreich A, Talanian RV, Sekul R, Kraft R, Thole H, Ottleben H, et al. Targeting of the transcription factor Max during apoptosis: phosphorylation-regulated cleavage by caspase-5 at an unusual glutamic acid residue in position P1. *Biochem J* 2001;358(Pt 3):705–15.
 51. Wang G, Ahmad KA, Ahmed K. Role of protein kinase CK2 in the regulation of tumor necrosis factor-related apoptosis inducing ligand-induced apoptosis in prostate cancer cells. *Cancer Res* 2006;66:2242–9.
 52. Yabuki M, Tsutsui K, Horton AA, Yoshioka T, Utsumi K. Caspase activation and cytochrome c release during HL-60 cell apoptosis induced by a nitric oxide donor. *Free Radic Res* 2000;32:507–14.
 53. Litchfield DW. Protein kinase CK2: structure, regulation and role in cellular decisions of life and death. *Biochem J* 2003;369:1–15.
 54. Barve RA, Minnerly JC, Weiss DJ, Meyer DM, Aguiar DJ, Sullivan PM, et al. Transcriptional profiling and pathway analysis of monosodium iodoacetate-induced experimental osteoarthritis in rats: relevance to human disease. *Osteoarthritis Cartilage* 2007;15:1190–8.